Catalysis Science & Technology

Accepted Manuscript

ROYAL SOCIETY OF CHEMISTRY

www.rsc.org/catalysis

Catalysis
Science & Technology

RSC Publishing

PAPER

Phosphine free SBA-15-EDTA-Pd highly active recyclable catalyst: Synthesis Characterization and application for Suzuki and Sonogashira reaction

Cite this: DOI: 10.1039/x0xx00000x

Received ooth January 2012,
Accepted ooth January 2012

DOI: 10.1039/x0xx00000x

www.rsc.org/

Priti Sharma, A.P.Singh

Phosphine obstructed highly efficient and reusable SBA-15-EDTA-Pd(11) has been synthesized by anchoring Pd-EDTA complex over the surface of organo-functionalized SBA-15. The physiochemical properties of the organo-functionalized catalyst were analyzed by elemental analysis, ICP-OES, XRD, N_2 sorption measurement isotherm, TGA & DTA, solid state ^{13}C, ^{29}Si NMR spectra FT-IR, XPS DRS UV-Visible, SEM and TEM. XRD and N_2 sorption analyses of synthesized catalyst confirm that ordered mesoporous channel structure was retained even after the multistep synthetic procedures. The (100), (110) and (200) reflections in SBA-15 provide good structural stability, existence of long range order and high pore wall thickness. TGA-DTA results reveal that thermal stability of synthesized catalyst SBA-15-EDTA-Pd(11) maintained at higher temperature. The organic moieties anchored over the surface of SBA-15 and inside the pore wall were demonstrated by solid state ^{13}C NMR spectra and FT-IR spectroscopy. Further, solid state ^{29}Si NMR spectroscopy provides the information about degree of functionalization of surface silanol groups, of SBA-15 with organic moieties. The electronic environment and oxidation state of Pd metal in SBA-15-EDTA-Pd(11) were monitored by XPS, DRS UV-visible techniques. Moreover, the morphologies and topographic information of synthesized catalyst were confirmed by SEM and TEM spectroscopy. The synthesized catalyst SBA-15-EDTA-Pd(11) was screened for the Suzuki and Sonogashira coupling reactions show higher catalytic activity with higher TON (turn over number). The anchored solid catalyst can be recycled efficiently and reused several times (five times) without major loss in reactivity.

Introduction

Various homogenous complexes were widely used for organic transformation; however, separation and recycling of the rather expensive catalyst impart difficulties. Heterogenization of such homogenous catalysts on solid supports can mitigate these problems. Furthermore, heterogeneous catalysts have clear advantages over their homogeneous counterparts, which can be easily separated from the reaction medium. "Heterogeneous catalytic system includes polymer/dendrimer supported palladium catalysts palladium on carbon palladium supported metal oxides clays and molecular sieves.[1]" Since the synthesis of ordered mesoporous materials in 1992 sparked worldwide interest in the field of heterogeneous catalysis and separation science; SBA-15 has become the most popular member of the group possessed extremely high surface areas, easily accessible, uniform pore sizes and stability.[2]

To extent the applicability of SBA-15 materials, it is necessary to modify the surface by organic functional groups for anchoring metals and metal complexes. Grafting of functional organosilanes by using surface hydroxyl groups as anchor points has been widely used. Furthermore the leaching of the active site can also be avoided as the organic moieties are covalently attached to the inorganic support.

Palladium complexes with or without phosphine ligands can catalyze the C-C coupling reactions. The phosphine-assisted approach is the classical and well-established methods[3]. Which gives excellent results in a majority of cases; whereas phosphine ligands are expensive, toxic, and unrecoverable and also a major drawback of the phosphine ligands in a catalytic reaction is the oxidation of phosphine to a phosphine oxide as well as cleavage of the P-C bond, causing degradation of the catalytic cycle. In large-scale industrial applications, the phosphines might be a more serious economical burden than even palladium itself, which can be recovered at any stage of production or from wastes. Therefore, the development of phosphine-free catalysts for C-C bond-forming reactions would be an important topic of interest of the current industrial research.[4]

The accurate selection of the ligands for the complex synthesis is the key factor for the synthesis of the complex. Recently a number of nitrogen base compounds in phosphine free condition were commonly used as a ligand such as C based heterocyclic carbenes, C-N based 2-aryl-2-oxazolines, aryl (hetroaryl) oximes, arylimines, N, N-based diazobutadienes, DMG and salen complexes.[5] However, these ligands are not easily available and contain tedious and expensive synthesis processes and hardly stable in catalytic systems. Therefore, simple easily accessible stable catalyst is desired for the high temperature reactions.

Cross coupling reactions are one of broadest area for the synthesis of symmetrical and unsymmetrical binary compounds, which are the key components of the several natural products as well as in the field of engineering materials, such as conducting polymers, molecular wires and liquid crystals.[6] Among the basic types of palladium catalyzed transformations, Suzuki and Sonogashira reactions related chemistry occupied a special place.[7] The Suzuki cross-coupling reaction of organoboron reagents with organic halides represents one of the most versatile and straightforward methods for carbon-carbon bond formation. The reaction is largely unaffected by water, tolerating a large range of functionality and yielding non-toxic by-products. Furthermore, Sonogashira coupling of phenyl acetylenes and aryl halides is one example of palladium catalyzed reaction that allows connecting a C≡C triple bond substituent in an aromatic ring.

In 2005, Korolev et. al. described the synthesis of $PdCl_2$–EDTA complex is homogeneous catalyst for the Suzuki–Miyaura reactions in water[8]. However, this catalytic system was not stable enough to store for longer time period and unfortunately, no catalyst recovery was possible. In this context, we decided to immobilize the Pd-complex the surface of organo-functionalized SBA-15 in order to recycle the catalyst. Herein, we report grafting of Pd-EDTA complex, and its derivatives into SBA-15 phases and their catalytic properties in Suzuki and Sonogashira coupling reactions as heterogeneous catalyst. The immediate goals of our study were (i) to evaluate the heterogenization method of the Pd-Ethylenediaminetetraacetic acid complex over organo-modified mesoporous SBA-15 support, (ii) to measure the catalytic properties in Suzuki and sonogashaira C-C coupling reaction (iii) to optimize the reaction parameter such as temperature, solvent and base in the both coupling reaction, (iv) to determine the extent stability of the catalysts as well as their recycling properties.

Results and Discussion

The heterogenized palladium catalyst SBA-15-EDTA-Pd was obtained by the procedure outlined in Scheme 1. Starting from the synthesis of SBA-15 and Surface modification was achieved by a post synthesis grafting method (scheme 1A) furthermore, free -OH groups present in NH_2-SBA-15 were protected (scheme 1B) by published procedure.[21] Finally Pd-EDTA complex was covalently grafted over the organo-modified surface of the SBA-15.[8] The products were dried and characterized systematically by nitrogen sorption isotherms; cross polarization magic angle spinning (CPMAS) NMR and infrared spectroscopies; elemental analysis; and thermogravimetric and differential thermogravimetric (TGA-DTA) analysis to gain complete structural and compositional information.

XRD pattern of (a) calcined SBA-15, (b)-OH protected NH_2-SBA-15 and (c) Pd-EDTA-SBA-15(11) complexes are visualized in Figure 1 and (a) SBA-15-EDTA-Pd(7), (b) SBA-15-EDTA-Pd(11), (c) SBA-15-EDTA-Pd(15) in Figure S1(see supporting information). The typical hexagonal phase of the SBA-15 [main (100), (200), and (210)] reflections are clearly visible in calcined SBA-15. In all the samples, (110) reflection is more intense than the (200) reflection. It favors more complete condensation of the wall structure due to the higher temperature preferring at hydrothermal synthesis and further calcinations. As evident from the figure 1 the XRD patterns of the samples synthesized after treatment with 3-APTMS and $[(MeO)_2SiMe_2]$ are almost similar to the parent SBA-15 sample with small decrease in overall intensity to the (100), (110) and (200) reflections. From the XRD pattern it is clear that after anchoring of Pd-EDTA complexes with different weight % ratio (7%, 11%, 15%) an inconsequential decrease in peak intensities to the (100), (110) and (200) reflections were observed without changing the peak positions (Figure S1). This perseverance of peak positions indicates that, even the presence of a large amount of Pd-EDTA complex moieties by the partial filling inside the mesopores is less detrimental to the quality of the SBA-15 material.[9] The persistence of the (100), (110) and (200) reflections (Figure 1) not only proved the structural stability and existence of long range ordering to the mesophase but also the survival of undisturbed pore wall thickness even after a number of treatments with organic molecules in solvents.

The nitrogen adsorption-desorption results of calcined SBA-15 and SBA-15-EDTA-Pd(7), SBA-15-EDTA-Pd(11), SBA-15-EDTA-Pd(15) samples and their corresponding pore size distribution curves are plotted in Figure 2 & S2, respectively. N_2 adsorption-desorption isotherms of all the samples show Type IV isotherms. The surface area, average pore diameter, pore volume and wall thickness were observed for the calcined SBA-15 and SBA-15-EDTA-Pd(7), -11 and -15 derivatives samples are summarized in the Table 1. All samples show type IV adsorption isotherms, according to the IUPAC classification, indicating the uniformity of the mesopores due to capillary condensation of N_2 within the mesopores with completely reversible nature, uniformly sized mesopores, with a capillary condensation step at P/P_o = 0.3-0.4.

The total surface area, average pore diameter and pore volume observed for the calcined SBA-15, SBA-15-EDTA-Pd(7), SBA-15-EDTA-Pd(11) and SBA-15-EDTA-Pd(15) were found to be 739 m^2g^{-1}, 65Å, 1.173 cm^3g^{-1}, 665 cm^3g^{-1}, 64.3Å, 0.439 cm^3g^{-1}, 363 m^2g^{-1}, 56 Å, 0.478 cm^3g^{-1} and 187 m^2g^{-1}, 48.5 Å, 0.36 cm^3g^{-1}, respectively. The decrease in total mesoporous surface area (10%, 50%, 74%), pore diameter (2%, 13%, 26%) and pore volume (62%, 59%, 69%) after metal Pd-EDTA complex immobilization over organo-modified SBA-15 is indicative of the grafting of complex Pd-EDTA inside the channels of mesoporous SBA-15. It is clear from Table 1 that even though silylation procedures changed the textural properties of the mesoporous material, the decrease is more prominent after Pd-EDTA complex immobilization since the bulkier organic moieties inside the pore channels occupies a large area of the void space. The capillary condensation steps of

SBA-15-EDTA-Pd(7), SBA-15-EDTA-Pd(11), and SBA-15-EDTA-Pd(15) due to anchoring of Pd-EDTA complexes get reduced to lower *P*/*P*o values. The shift to slightly lower partial pressure shows possible reduction in the pore size and a partial distortion in pore arrangement, consistent with the XRD results. It is known that the inflection position in N_2 sorption isotherms depends on the diameter of the mesopores and the sharpness usually indicates the uniformity of the mesopores, due to capillary condensation of N_2 within the mesopores.

The presence of isolated surface silanols, hydrogen bonded hydroxyl groups, anchored complex Pd-EDTA are evidenced from the IR spectrum of the calcined SBA-15 and its modified samples. Figure 3 shows FT-IR spectra of (a) EDTA, (b) calcined SBA-15, (c) –OH protected NH_2-SBA-15, (d) SBA-15-EDTA-Pd(7), (e) SBA-15-EDTA-Pd(11), (f) SBA-15-EDTA-Pd(15). In the visualized IR spectrum of calcined SBA-15 and –OH protected NH_2-SBA-15 the ν-OH stretching vibrations observed in the range of 3600–3400 cm^{-1} region are attributed to the hydrogen-bonded silanol groups and the sharp band at 3757 cm^{-1} corresponds to the isolated surface silanol groups (Figure 3b) In the present analysis, after 3-APTMS functionalization, a sharp decrease in the intensity of peak at 3757 cm^{-1} with a peak shift to lower value is seen, demonstrating the role of surface silanols in modifications (Figure 3c). In Figure 3 the band observed near 797 cm^{-1} and 1076 cm^{-1} are due to the symmetric and asymmetric vibrations of the Si-O-Si group, respectively.[10] Two strong bands were observed in the case of SBA-15-EDTA-Pd(11) complexes at 1620 and 1587 cm^{-1}; corresponds to the C-O stretching vibrations and N-H bending vibrations, respectively.[11] Further, the intensity of the C-O stretching vibrations and N-H bending vibrations increases as the loading of Pd-EDTA complex increases. Since the Pd-EDTA was anchored over the modified surface of the SBA-15, the band at 3294 cm^{-1} ascribed to the NH_2 stretching vibrations disappeared, while a broad weak band at 3257 cm^{-1} was observed, which is attributed to the stretching vibration of –[NH_3]+ resulted from the EDTA modification.[12] This broad band shows much broader in case of SBA-15-EDTA-Pd(15) catalyst, which might be due to higher loading of Pd-EDTA complex. Further, new bands at 1383 and 1627 cm^{-1} were also observed for Pd-EDTA modified SBA-15 which attribute to the -COO- group symmetrical and asymmetrical stretching vibrations, respectively. These observed results indicate that all the SBA-15-EDTA-Pd complexes along with different loading are systematically synthesized.

Figure 4 show the solid state ^{13}C CP/MAS NMR spectra of (a) NH_2-SBA-15, (b) –OH protected –NH_2-SBA-15, (c) SBA-15-EDTA-Pd(11). In the solid state ^{13}C CP/MAS NMR spectra of NH_2-SBA-15, -OH protected NH_2-SBA-15 and SBA-15-EDTA-Pd(11) the peak observed at 9.3 ppm can be accounted for carbon (C1) atom bonded to the silicon. The signal at 21.3 ppm corresponding to methylene carbon (C2) and signal at 42.5 ppm can be attributed to the carbon atom attached to NH_2 group (Figure 4a). After -OH group protection of NH_2-SBA-15 by dimethoxydimethylsilane along with all three peak of NH_2-SBA-15, one extra peak is clearly visible at -2.2 ppm corresponds to methyl group attached to capping agent dimethoxydimethylsilane (Figure 4b). And no peak was observed for the methoxy group which confirms the successful grafting of 3-APTMS over the support (SBA-15). Two consecutive peaks observed at 171 ppm and 180.6 ppm corresponds to the carbon atoms of the amide group formation due to the carboxylic group get anchored to the linker 3-APTMS of the SBA-15. Furthermore, another peak observed in the case of SBA-15-EDTA-Pd(11) at 63.85 ppm corresponds to the carbon of ethylene group in EDTA, which is directly attached to the amide group and peak at 55.4 ppm is due to ethylene group which is directly attached to carboxylic acid group (Figure 4c). The reason of appearance of two type peaks of carboxylic acid peaks might be the all carboxylic group did not get anchored over the 3-APTMS modified surface of the SBA-15.

^{29}Si MAS NMR spectra of (a) Calcined SBA-15, (b) NH_2-SBA-15, (c) -OH protected-NH_2-SBA-15, (d) SBA-15-EDTA-Pd(11) exhibited in Figure 5. Demonstrated peaks in spectra at -112, -102, -68 and -61 ppm which are usually assigned to Q^4 [$Si(OSi)_4$, siloxane], Q^3 [$Si(OH)(OSi)_3$, single silanol], and sites T^3 [$SiR(OSi)_3$], respectively (Figure 5a,b,c,d). The calcined SBA-15 sample shows the presence of broad resonance peaks from -126 to -98 ppm, indicative for a range of Si-O-Si bond angles, and it is noteworthy that the sample contains large amounts of Q^4 sites showing a high framework cross-linking.[13] The low intensity in the Q^3 value shows that these silanol groups are highly accessible to the silylating agents (Figure 5a). In -OH protected-NH_2-SBA-15, Si spectrum shows one extra peaks at -68.48 ppm due to capping agent dimethoxydimethylsilane, which are assigned to mixture of T^3 [$SiR(OSi)_3$] and T^2 [$Si(OH)R(OSi)_2$] organosilicon, respectively. Peak at -16.87 ppm corresponds to Si of (dimethoxy dimethylsilane) capping agent (Figure 5c). After protection of -OH group in NH_2-SBA-15 by dimethoxydimethylsilane, it is clearly visible that T^2 site [$Si(OH)R(OSi)_2$] disappeared along appearance with new peak at 16 ppm. With these two significant changes evidently proved the free silanol group of NH_2-SBA-15 the T^2 site [$Si(OH)R(OSi)_2$] get blocked by the condensation with methoxy group of dimethoxydimethylsilane (Figure 5c). The absence of T^o($SiC(OH)_3$ sites confirms the EDTA-Pd complex is covalently anchored to the modified surface of the SBA-15 (Figure 5d).

Thermal stability of all the synthesized materials were studied by thermo gravimetric analysis under air atmosphere from ambient temperature to 1000°C with a temperature increment of 10°C/min. TGA plots of all synthesized and modified SBA-15 samples show approximately 5% weight loss below 120°C caused by the desorption of physiosorbed water molecules (Figure S3). In TGA plot loss of ~42 weight % from as-synthesized SBA-15 was observed between 132°C and 195°C; corresponds to the removal of trapped surfactant within closed pore (Figure S3,A,B,a). Whereas nearly no weight loss in TGA and DTA was observed in the calcined SBA-15 between 132°C and 195°C indicate the complete removal of surfactant from SBA-15[14] (Fig.S3, A,B,b). These data evidently supports the complete removal of organic surfactant from calcined SBA-15. TGA result of -OH protected NH_2-SBA-15 sample shows weight loss in three steps. In the first step, weight loss between 70°C and 150°C corresponds to the loss of loosely bounded water, adsorbed moisture, which is clearly evidenced by the small exothermic peak of DTA. In the second step weight loss was observed in the region of 245°C-385°C. TGA analysis and a sharp visible exothermic peak in DTA analysis in the same temperature region (245°C-385°C) are attributed to 3-APTMS. TGA plot of -OH protected NH_2-SBA-15

quantitatively shows ~21.27% weight loss, which is greater than calcined SBA-15; strongly supports successful anchoring of 3-APTMS over SBA-15. Third weight loss visible in TGA analysis in 380°C-480°C range corresponds to removal of dimethoxydimethylsilane [$(MeO)_2SiMe_2$] which is evidently supported by DTA analysis showing one strong exothermic peak in the same temperature range (Fig.S3,B,c). In the case of heterogenized metal complex SBA-15-EDTA-Pd(11) one extra peak was observed along with two peaks shown in –OH protected NH_2-SBA-15, in the region of 437-556°C assigns Pd-EDTA complex. Note that decomposition of Pd-EDTA complex occurred at elevated temperature revealing the high thermal stability of complex. Direct comparison of weight loss in the case of heterogenized SBA-15-EDTA-Pd(11), and in capped amino functionalized SBA-15 shows ~7 weight % loading of complex material (Figure S3, A,B,d).

TEM image of calcined SBA-15 and SBA-15-EDTA-Pd(11) provide structural evidence that the material organized into ordered arrays of two-dimensional hexagonal mesopores (Figure 6). The significant difference of the TEM patterns was not observed between the two Figures 6A, B. However, after the anchoring the EDTA-Pd complex inside the mesoporous channels of SBA-15 the images had shown distinct deep contrasting meso parallel channels with respect to the light shaded surface. This might be interpreted as due to the presence of the EDTA-Pd complex inside the SBA-15, but not on the surface. If the EDTA-Pd complex was anchored on the surface of the functionalized SBA-15, then the high-contrast dark meso parallel channels would have appeared along the boundary of the visualized SBA-15 and not inside the porous body as observed previously by Shephard et al[15]. Thus, the immobilization of the Pd-complex inside the pore-channels, by anchoring to the interior walls of these porous channels may be supported by TEM.

Morphologies of the calcined SBA-15 and SBA-15-EDTA-Pd(11) are shown in Figure 7 A,B, respectively. Calcined SBA-15 shows uniform arrays of mesochannals arrangement and clearly molecular-scale periodicity in the SEM images. Further, SBA-15-EDTA-Pd(11) demonstrates molecular-based materials; the large molecular system becomes denser in comparison to the calcined SBA-15 after Pd-EDTA complex anchoring over the mesoporous surface.

X-ray photoelectron spectroscopy (XPS) is the powerful tool to investigate the electronic properties of the species formed on the surface, such as the electronic environment, e.g. oxidation state and or multiplicity influences in the binding energy of the core electron of the metal. The synthesized material SBA-15-EDTA-Pd(11) was characterized by X-ray photoelectron spectroscopy (XPS) to ascertain the oxidation state of Pd species. In Figure S4 (supporting information) the Pd binding energy of SBA-15-EDTA-Pd(11) exhibits two strong peak centered at 336.7 eV and 341.5 eV, respectively, which are assigned to the Pd $3d_{5/2}$ and Pd $3d_{3/2}$ signal, respectively. The observed peaks correspond to the Pd^{2+} oxidation state in the synthesized SBA-15-EDTA-Pd(11). According to literature pure $PdCl_2$ metal salt binding energy for Pd $3d_{3/2}$ and Pd $3d_{5/2}$ orbital appears at 342.8 and 337.6, eV, respectively.[16] In comparison to literature value, the synthesized SBA-15-EDTA-Pd(11) show shift in binding energy of Pd towards lower value viz 341.5 Pd $3d_{3/2}$ and 336.7 eV Pd $3d_{5/2}$, respectively.[17] The shift in the binding energy towards lower values indicated that the Pd state in SBA-15-EDTA-Pd had more electron rich state than $PdCl_2$. The reason might be possibility of electron donation from EDTA to Palladium and it suggested the strong interaction between Pd metal species and EDTA ligand was presence in SBA-15-EDTA-Pd catalyst. These results are in agreement with the UV-vis observations.

Diffuse reflectance UV-Vis measurement is a useful technique to get information about the oxidation state of incorporated metal species. The UV-Vis spectra of (a) Calcined SBA-15, (b) SBA-15-EDTA-Pd(7), (c) SBA-15-EDTA-Pd(11), (d) SBA-15-EDTA-Pd(15) are shown in Figure 8. Calcined SBA-15 shows the characteristic absorption at 254 nm, which corresponds to the siliceous material (Fig.8,a). The diffuse reflectance spectra (200–800 nm) of SBA-15-EDTA-Pd (Pd-EDTA loading 7, 11, 15%) catalysts display nearly identical features in absorption bands in the UV region in the range 205-680 nm with reference to $BaSO_4$ standard. The UV visible spectra of the SBA-15-EDTA-Pd (Fig 8, a, b, c) show the characteristics bands at 205-290 nm and 325-362 nm and broad peak at 682 nm. The weak bands in 205- 290 nm region assigned to the weak p-p* transitions (Figure 8, b, c, d). Bands in 325-362 nm regions assigned to the d-d transition of the metal[18]; strongly supports the Pd(II) oxidation state. Another band appears at the 682 nm which might be due to n-p* transition after incorporation of Pd-EDTA over the modified surface of the SBA-15.

Suzuki Coupling

The catalyst SBA-15-EDTA-Pd with different wt.% loading of Pd-EDTA (7%, 11%, 15%) were screened in the Suzuki coupling reaction using the following reaction conditions: arylboronic acid (1.5 mmol), aryl halide (1 mmol), potassium carbonate (3 mmol), DMF (3.5 ml), SBA-15-EDTA-Pd (15 mg) at 120°C. The conversion of iodobenzene and TON with respect to Pd loading were found to be 70%, 99%, 99% and 100, 130.2 and 74.2, respectively. The reaction proceeds at the active Pd metal centre. Further the TON increases from SBA-15-EDTA-Pd(7) to SBA-15-EDTA-Pd(11) thereafter decreases.

The heterogeneous Suzuki cross-coupling of boronic acid with aryl iodide may proceed through a catalytic cycle analogous to that proposed for homogeneous palladium catalysts[19]. In the first step of reaction insight, oxidative addition of aryl halide ArX (**2**) to the SBA-15-EDTA-Pd(11) **(1)** complex provides SBA-15 bound aryl palladium (II) complex (**3**). The leaving anion adds to the metal center to give the intermediate (**3**). The displacement of halide ion **(X)** from SBA-15-L-(Ar–Pd–X) **(3)** to give the more reactive organopalladium alkoxide SBA-15-L-(Ar–Pd–CO_3K^+) or organopalladium hydroxide (R–Pd–OH) depends on the base used. Further, in second step of reaction mechanism transmetalation between SBA-15-L-(Ar–Pd–CO_3K^+) aryl palladium (II) complex **(6)** and bornonic acid **(7)** provides SBA-15-L-(Ar^l-Pd-Ar) reaction intermediate **(10)** with the subsequent removal of byproduct $B(OH)_2(CO3\ K^+)_2$ (**9**). In the last step of reaction mechanism; with reductive elimination of biphenyl Ar^l-Ar (**11**) from the unsymmetrical Intermediate (**10**) regenerates the SBA-15-L-Pd **(1)** complex.

Since mechanism of Suzuki coupling reaction is multistep procedure and a small variation in physical and reaction parameter can change the product yield and rate of the reaction

drastically. Hence the influences of solvent, reaction temperature and various bases were evaluated on the product yield using SBA-15-EDTA-Pd(11) as catalyst in iodobenzene and boronic acid.

In order to probe the role of solvents in Suzuki coupling reaction, series of solvent like DMSO, DMF, HMPA, THF, 1,4 dioxane, and toluene were used in presence of base potassium carbonate (K_2CO_3) at 120ºC in a model reaction of suzuki coupling between iodobenzene and boronic acid. Among all the used solvents DMF, DMSO and NMP were able to give a significant yield (85-100%) in 5 h reaction time period (Figure S5). whereas the nonpolar or less polar solvent such as THF, toluene progress with strong reason of intermediate stabilization via coordinating ability and the polarity. From the obtained results of solvent optimization for the conversion of iodobenzene the reactivity order emerged as follows: DMF (100%) > DMSO (89%) > NMP (83%) > THF (39%) > Toluene (17%) > 1,4 dioxane (15%) > Xylene (10%), respectively (Figure S5). In addition, the conversion of iodobenzene was also carried out using SBA-15-EDTA-Pd(11) in presence of water as solvent under the similar reaction conditions. The yield of the biphenyl was found to be 33 wt.% in 12 h reaction time. Since after oxidative addition of aryl halide charge separation would take place at Pd metal centre to a much greater extent. To stabilize the generated high charge during the oxidative step at the Pd centre more coordination required which is possibly by the high polar solvents. Suzuki coupling reaction of iodobenzene (1 mmol) and boronic acid (1.5 mmol) in presence of K_2CO_3 using solvent DMF (3.5 ml) over SBA-15-EDTA-Pd(11) (15 mg) catalyst was examined to see the influence of temperature in the range of 60ºC to 120ºC on the product yield (Figure S6). Lower temperature does not favour the formation of product (biphenyl); however the yield of biphenyl increased sharply with the increase in reaction temperature and reached the value of 99% in 6 h at 120ºC. Generally, coupling reaction favoured at high temperature since high activation energy is required to dissociate the aryl halide bond at oxidative addition step. It is noteworthy to mention here that no biphenyl product was obtained below 55°C. Hence, the optimum reaction temperature with respect to conversion towards biphenyl product, under present reaction conditions, was found to be 120ºC (Figure S6).

Various bases such as NaOH, $NaHCO_3$, K_2CO_3 and NEt_3 were screened for the reaction. Among all used bases organic bases like triethyl amine (NEt_3) was found unreactive in comparison to inorganic bases. The order of reactivity of iodobenzene in presence of various bases is arranged in the decreasing order as: K_2CO_3 (100) > NaOH (60) > $NaHCO_3$ (45) > > NEt_3 (32). It is clear that the reactivity of K_2CO_3 is found to be quite high among the used inorganic bases (Figure S7). Potassium carbonate is able to give 95% yield of coupled product (biphenyl) in 5 h at 120°C. Suzuki coupling reaction is known to be affected by salt particles, yet their mode of action has not been completely clarified. According to the one hypothesis.[20] in the reaction, the anions at the surface of the solid salt particles acted as electron donors for Pd metal centre, which increased the electron density of Pd metal centre. This effect could promote the oxidative step to form intermediate Ar–Pd-X **(3)**. Therefore, the reaction is accelerated because this is the rate determining step. In other words, the electron-donation effect could enhance the activity of the catalyst with the increase in electron density of Pd.

The characteristics of organoboron reagents (i.e., high selectivity in cross-coupling reactions, stability, nontoxic nature, and tolerance towards functional groups) often give the Suzuki coupling a practical advantage over other cross-coupling processes. After optimizing the reaction parameters of the Suzuki coupling reaction between iodobenzene and phenyl boronic acid; several substituted and non-substituted aryl halides were employed in the reaction and the results are summarized in Table 2. The desired corresponding products are obtained in good yields with high TONs. As shown in Table 2, the Suzuki coupling reaction of phenyl boronic acid with variety of aryl halide proceeds smoothly under mild reaction conditions giving the corresponding coupled products in high yields (75% - 99%) (Table 2, entries 1-10).

Monosubstituted Aryl halides such as chlorobenzene, bromobenzene and iodobenzene with phenyl boronic acid gave 71%, 83%, 98% yield of biphenyl and corresponding TON were found to be 81.2, 94.9 and 128.9, respectively (Table 2, entries 1, 2, 3). In the step of oxidative addition of catalytic cycle of the halogenated (X = Cl, Br, I) substrates coupling reactions involving these substrates typically decrease in the order of R–Cl > R–Br > R–I. This can be explained in terms of the R–X bond dissociation enthalpies (BDE). For example, the X–Ph BDE range from X = Cl 95.5 ± 1.5 kcal/mol; X =Br 80.4 ± 1.5 kcal/mol to X= I 65.0 ± 1 kcal/mol. It is evident from the Table 2 that the reactivity of aryl chloride and bromides with phenyl boronic acid were found lower than aryl iodides and require comparatively longer reaction times for the completion of reaction.

Furthermore, electron rich and electron poor aryl halides react smoothly with phenyl boronic acid in the similar reaction conditions. Electron poor aryl halides like 4-chloronitrobenzene, 4-bromonitrobenzene and 4-iodonitrobenzene with phenyl boronic acid gave coupled product (4-nitro biphenyl) in 98%, 99%, 95% with TON 128.9, 130.2, 125, respectively (Table 2, entries 4, 5, 6). The relative reactivity of aryl halide towards the metal centre decreases in the order: I > Br >> Cl. Aryl halides activated by the proximity of electron-withdrawing groups are more reactive to the oxidative addition than those with donating groups, thus allowing the use of electron deficient halides such as 4-chloronitrobenzene for the cross-coupling reaction. Further, aryl iodides are more reactive than the bromides and chlorides. The substituent effect in the aryl iodides appeared to be less significant than in the aryl chlorides and bromides.

Subsequently, the electron rich aryl halides also show moderate to excellent reactivity (89%-96% yield) in the formation of corresponding products (4-methylbiphenyl, 4-methoxybiphenyl) in Suzuki coupling reaction under the similar reaction conditions. The electron rich para substituted aryl halides such as 4-bromotoluene, 4-iodotoluene 4-bromoanisole with bornonic acid afford 96%, 94%, 89% yield after 9 h, 7 h, 9 h, respectively (Table 2, entries 7, 8, 9). The coupling reaction of chloronapthalene with phenyl boronic acid was investigated under similar reaction condition, but no desired coupled product was obtained even after 24 h of reaction time. In addition, the catalytic activity of SBA-15-EDTA-Pd(11) was compared with homogeneous counterpart. The product yield over SBA-15-EDTA-Pd(11) and EDTA-Pd were found to be 98 and 99 wt.% conversion in 5 h and 1 h, respectively (Table 2, entries 3 and 10).

Sonogashira Reactivity

The original Sonogashira reaction often required highly dry organic solvent, inert atmosphere, highly strong base, prolonged reaction time and phosphine containing catalyst. Generally a copper co-catalyst is needed in Sonogashira coupling reaction. However, the addition of copper, although beneficial in terms of increasing the reactivity of the system, added some shortcomings, the principal being the necessity of avoiding the presence of oxygen in order to block the undesirable formation of alkyne homocoupling through a copper mediated Hay/glasier reaction. The coppper-acetylides formed in-situ could undergo oxidative dimerization to give diaryldiacetylenes when they are exposed to air or an oxidant (a reaction known as the Glaser coupling). These byproducts are generally difficult to separate from the desired products. Furthermore, the copper acetylide is a potential explosive reagent. To address such a problem, a solution was to eliminate the copper in the so-called ''copper-free'' Sonogashira reaction.[21]

Here we have shown that the synthesized catalyst SBA-15-EDTA-Pd(11) catalyst is efficient to handle in phosphine and copper free conditions for Sonogashira coupling reaction. Without the involvement of copper there are even fewer mechanistic suggestions to be found in homogeneous catalytic system.[22] The heterogeneous Sonogashira coupling of phenyl acetylene with aryl halide may proceed through a catalytic cycle analogous to that proposed for homogeneous palladium catalysts.

In the first step the catalytic cycle is initiated by oxidative addition of the aryl halide (Ar-X) to species **(1)**, forming the oxidative addition adduct reaction intermediate **(2)** species. The second step is the activation of the terminal alkyne. Because no copper salt was employed, and the base must be strong enough to subtract a proton from the alkyne, a transmetalation step could be excluded.[21] The terminal alkyne C-H bond activation is accomplished by the coordination of the alkyne to SBA-15-L-(Ar^I-Pd-X) **(3)** complex. Upon coordination, the C-H bond is weakened, and H-X is removed from SBA-15-L-(Ar^I-Pd-X) **(3)** in the presence of a base (Triethylamine) **(6)** to form reaction intermediate **(5)** with the subsequent byproduct of triethylaminehalide **(7)**. In the last step of reaction mechanism; with reductive elimination of diphenylacetylene Ar^I-Ar **(7)** from the unsymmetrical Intermediate **(6)** regenerates the SBA-15-L-(Pd) complex.[21]

In order to probe the role of solvent in the Sonogashira coupling reactions a series of various bases such as NaOH, Na_2CO_3, K_2CO_3, NEt_3 and $NaHCO_3$ were screened for the reaction.[21] Among all used base organic base like triethylamine (NEt_3) was found most reactive in comparison to inorganic bases. The order of reactivity of Iodobenzene in presence of various bases is arranged in the decreasing order as: NEt_3 (100%) > K_2CO_3 (58%) > Na_2CO_3 (45%) > NaOH (35%) > $NaHCO_3$ (10%). It is clear from the comparison that triethylamine base plays a highly active role in Sonogashira coupling reaction (Figure S8). These organic bases were superior to inorganic bases such as K_2CO_3, Na_2CO_3, NaOH, $NaHCO_3$, and NEt_3. This may be due to the partial inhomogeneity of inorganic bases with the organic substrate, reagent, and solvent, which lowered the conversion and increased the reaction times compared to organic bases (10-100% in 2 h).

After optimizing the reaction parameters, various substituted and non substituted aryl halide are also investigated in the Sonogashira coupling reaction between iodobenzene and phenyl acetylene in Cu free reaction conditions and results are summarized in Table 3.

Various aryl halides were coupled with phenylacetylene in presence of SBA-15-EDTA-Pd(11), triethylamine (3 mmol) and DMF as solvent at 120°C (Table 3). As evident from the Table 3 all substituted and non substituted aryl halides react with phenyl acetylene under mild reaction conditions to give their corresponding products (Table 3, entries 1-8). Mono substituted aryl halides such as chlorobenzene, bromobenzene and iodobenzene with phenyl acetylene gave coupled product (biphenyl) in 75%, 85%, 100% yield with TON 85, 97, 114, respectively. As discussed earlier, chlorides show poor reactivity compared to bromides and iodides under similar reaction conditions. As clear from the Table 3, Sonogashira coupling reactions coupled fast with the aryl iodides and bromides in comparison to chlorides (Table 3, entries 1, 2, 3).

Electron withdrawing (deficient) nitro (-NO_2) bearing aryl halide such as 4-chloronitrobenzene, 4-bromonitrobenzene, 4-iodonitrobenene with phenyl acetylene gave coupled product 4-nitrobiphenyl in 99%, 98%, 100% yield and 113, 112, 114 TON, respectively. From the catalytic cycle point of view in Sonogashira coupling reaction, oxidative addition of aryl halide to Pd metal centre results into transition state (**3**) in the first step. The relative reactivity decreases in the order of I > Br >> Cl. Aryl halides activated by the proximity of electron-withdrawing groups are more reactive to the oxidative addition than those with donating groups. Electron withdrawing groups increase the reactivity of aryl halides in coupling reaction; which is clear from the Table 3 (entries 4, 5, 6). However, the electron donating group such as Methyl bearing aryl halides such as 4-bromotoluene, 4-iodotoluene with phenylacetylene gave corresponding products in 89%, 99% yield with 101, 113 TON, respectively (Table 3 entries 7, 8).

Generally electron donating bearing Aryl halides show less reactivity in coupling reaction as the electron density increases over the Pd intermediate **(3)** results into lower feasibility for further transmetalation and reductive elimination step, respectively. It is clear from the Table 3 (entries 5-8) that aryl halides bearing methyl, nitro groups react with phenyl acetylene to give excellent yields of the corresponding biaryl; whereas the aryl chloride possessed pera-substituents, give good yields. Electron-rich substrates such as 4-bromotoluene and 4-iodotoluene show lower reactivity in comparison to the electron withdrawing bearing aryl halides and take longer reaction time period for completion of the reaction (Table 3, entries 7, 8). The coupling reaction of sterically hindered 2-chloronapthalene with phenyl acetylene did not proceed even after longer reaction time (24 h).

Heterogeneity and Recycling studies of Catalyst SBA-15-EDTA-Pd(11)

To test if metal was leached out from the solid catalyst during reaction; the hot filtration test was performed. In this

process the Sonogashira coupling reaction mixture was collected by filtration at the reaction temperature (120°C) after a reaction time of 1 h which gave 58% conversions of iodobenzene. The residual activity of the supernatant solution was studied. It was noticed that after filtration of the SBA-15-EDTA-Pd(11) catalyst from the reaction mixture at the elevated reaction temperature (120°C) (in order to avoid possible recoordination or precipitation. of soluble palladium upon cooling) coupling reactions did not proceed further. Thus results of the hot filtration test suggest that Pd was not being leached out from the solid catalyst during the coupling reactions. These results confirm that the palladium catalyst remains on the support even at elevated temperatures during the reaction.

Further, to evaluate the reusability, after carrying out the reaction, the mixture was filtered using a sintered glass funnel, and the residue washed with DMF (3-5 ml), dichloromethane (2-5 ml) and acetone (2-5 ml). After being dried in an oven (overnight), the catalyst could be reused directly without further purification (Figure 9). The amounts of Pd leaching into solution for the Suzuki reactions were detected through ICP. The loss of Pd amount for reaction was less than 1.0 weight % of total Pd content. Even though a small amount of Pd loss could be detected, catalyst still showed relatively high reusability and stabilities reusability and stabilities for Sonogashira coupling reactions. The present study indicates that the catalyst can be recycled a number of times without losing its activity to a greater extent.

Conclusion

In summary, highly stable and recyclable SBA-15-EDTA-Pd catalyst has been synthesized by anchoring Pd-EDTA complexation over the inner surface of organo-functionalized SBA-15 different wt.% loading (7%, 11%, and 15%). XRD and N_2 sorption analyses which reveals that morphological and textural properties of synthesized catalyst confirm that metal complex Pd-EDTA are firmly attached to the organo-modified SBA-15 support and the ordered mesoporous channel structure was retained even after the multistep synthetic procedures. TGA-DTA results reveal the thermal stability of synthesized catalyst SBA-15-EDTA-Pd(11) at elevated temperature. The organic moieties anchored over the surface of SBA-15 and inside the pore wall were evident by solid state ^{13}C NMR spectra and FT-IR spectroscopy. Further solid state ^{29}Si NMR spectroscopy provides the information about degree of silylation and functionalization with organic moieties. The electronic environment and oxidation state of Pd metal in SBA-15-EDTA-Pd(11) were confirmed by XPS, DRS UV-visible techniques. Subsequently, the morphologies information of synthesized catalyst was monitored by SEM and TEM spectroscopy. The synthesized heterogeneous catalyst SBA-15-EDTA-Pd(11) screened in the Suzuki and Sonogashira coupling reaction and shows higher catalytic activity with higher TON in phosphine free conditions. The present SBA-15-EDTA-Pd(11) catalytic system tolerates a broad range functional group of aryl halide in both Suzuki and Sonogashira coupling reaction without using phosphine ligand or Cu co-catalyst. The heterogenized solid catalyst SBA-15-EDTA-Pd(11) can be recycled efficiently and reused five times without major loss in activity due to well modified surface properties of SBA-15 as a support.

Experimental

SBA-15 was synthesized according to the reported procedure using tri-block P123 as a template under acidic conditions.[23] Pluronic 123 (2 g) was dissolved in a solution of HCl (60 mL of 2.0 M) and H_2O (60 mL). The solution was stirred at 38ºC for 1 h. After that time, tetraethylorthosilicate (TEOS) was added, and the resultant solution was left stirring at 38ºC for further 4 h and then aged at 100ºC for 24 h. Surface medication (see supporting information)

SBA-15-Pd-EDTA Synthesis

$PdCl_2$ (0.5 mmol) in 5 ml distilled water was treated with 0.186 g (0.5 mmol) of EDTA and 1 mmol of sodium carbonate (Na_2CO_3) and stirred to give yellow red solution. To the resultant solution the calculated amount (1.0 g) of organo-modified SBA-15 was added along with the slow addition of 25 ml of Millipore water.[8] The final mixture was stirred at 75°C for 24 h and washed with distilled water and soxhlet extracted to remove the unanchored materials from the SBA-15 surface (scheme. 1D). The resultant material named SBA-15-EDTA-Pd(11). Similarly 7 and 15 wt.% of Pd loading were also synthesized by using corresponding amount of modified SBA-15 and $PdCl_2$ and obtained materials were designated as SBA-15-EDTA-Pd(7), SBA-15-EDTA-Pd(11), SBA-15-EDTA-Pd(15).

General procedure for Suzuki coupling reactions

Suzuki reaction was carried out in 25 ml oven dried two neck round bottom flask heated over reactor with high stirring 700+ rpm. In a typical run 1mmol of aryl halide, 1.15 mmol of aryl boronic acid, 3 mmol potassium carbonate (K_2CO_3) and 15 mg of SBA-15-EDTA-Pd(11) (heterogeneous catalyst) were allowed to stir at 120°C with solvent DMF (3.5 ml). The reaction mixture was sampled at measured time intervals and analyzed by gas chromatography. The samples were centrifuged with high rpm before injecting in gas chromatography.

General procedure for Sonogashira coupling reactions

Catalyst screening for Sonogashira coupling reaction was carried out in 25 ml oven dried two necked round bottom flask heated over reactor with high stirring 700+ rpm. In a typical run 1mmol of aryl halide, 1.5 mmol of phenylacetylene, 3 mmol triethylamine (base) and 15 mg of SBA-15-EDTA-Pd(11) (heterogeneous catalyst) were allowed to run at 120°C with DMF as solvent. The reaction mixture was sampled at measured time intervals and analyzed by gas chromatography. The samples were centrifuged with high rpm before injecting in gas chromatography. The products were analyzed by GCMS and ^1H, ^{13}C CP MAS NMR.

Acknowledgements

Author gratefully acknowledges the CSIR networking project (CSC-0125) for financial support. P.S. thanks UGC-New Delhi, India for Senior Research Fellowship. Authors are thankful to Dr. Satynarayana chlikuri for adsorption measurements (surface area) and Dr. Vinod for the XPS studies.

A.P.Singh.
Catalysis Division
CSIR-National Chemical Laboratory
Pune 411008, India
Fax: (+) 91 20 2590 2633
Tel: (+) 91 20 2590 2497
E-mail: ap.singh@ncl.res.in (Dr. A. P. Singh)

Electronic Supplementary Information (ESI) available: [Suzuki, sonogashira product ^{1}H, ^{13}C NMR, details of experimental section, Pore size distribution plot, TGA, DTA plot, X-ray photoelectron spectroscopy (XPS), Solvent, Temperature and base optimization for the suzuki and sonogashira coupling reaction]. See DOI: 10.1039/b000000x/

Notes and references

[1] a) A. Dahan and M. Portnoy, *Org. Lett*. 2003, **5**, 1197-1200; b) F.X. Felpin, T. Ayad and S. Mitra, *Eur. J. Org. Chem*. 2006, **12**, 2679-2690; c) A. Cwik, Z. Hell and F. Figueras, *Adv. Synth. Catal*. 2006, **348**, 523-530; d) B. M. Choudary, S. Madhi, N.S. Chowdari, M. L. Kantam and B. Sreedhar, *J. Am. Chem. Soc*. 2002, **124**, 14127-14136.

[2] a) J. Y. Ying, C. P. Mehnert and M. S. Wong, Angew. Chem. Int. Ed. 1999, **38,** 56-77; b) D. Zhao, J. Feng, Q. Huo, N. Melosh, G. H. Fredrickson, B. F. Chmelka and G. D. Stucky, *Science*. 1998, **279**, 548- 552; c) R. I. Kureshy, A. H. Khan, K. Pathak and V. Jasra, *Tetrahedron: Asymm.* 2005, **16,** 3562-3569.

[3] a) C. Amatore, A. Jutand, M. Amine and M. Barki, *Organometallics* 1992, **11**, 3009-3013; b) H. A. Dieck and R. F. Heck, *J. Org. Chem* 1975, **40,** 1083-1090; c) C. A. Fleckenstein and H. Plenio, *Chem. Soc. Rev*. 2010 **39**, 694-711.

[4] a) A. Zapf and M. Beller, *Top. Catal* 2002, **19**, 101-109; b) L.X. Yin and J. Liebscher, *Chem. Rev*. 2007, **107,** 133-173.

[5] a) V. P. W. Bohm, C. W. K. Gstottmayr, T. Weskamp and W. Herrmann, *J. Organomet. Chem*. 2000, **595**, 186-190; b) B. Tao and D. W. Boykin, *Tetrahedron Lett*. **2002**, 43, 4955-4957; c) D. A. Alonso, C. Najera and M. C. Pacheco, *Org. Lett*. 2000, **2**, 1823-1826; d) B. Bedford and C.S. Cazin, *Chem. Comm*. 2001, **17**, 1540-1541; e) G. A. Grasa, A. C. Hillier and S. P. Nolan, *Org. Lett.* 2001, **3,** 1077-1080; f) S. R. Borhade and S. B. Waghmode, *Tetra. Lett.* 2008, **49**, 3423-3429.

[6] a) I. P. Beletskaya and V. Andrei, Cheprakov, *Chem. Rev*. 2000**, 100**, 3009-3066; b) V. Polshettiwar and A. Molnar, *Tetrahedron.* 2007, **63**, 6949-6976; c) S. P. Stanforth, *Tetrahedron.* 1998, **54**, 263-303.

[7] a) C. M. Crawforth, I. J. S. Fairlamb, A. R. Kapdi, J. L. Serrano, R. J. K. Taylor and G. Sanchez, *Adv. Synth. Catal.* 2006, **348**, 405-412; b) M. Lamblin, L. N. Hardy, J. C. Hierso, E. Fouquet and F. X. Felpin, *Adv. Synth. Catal.* 2010, **352**, 33-79; c) X. F. Wu, H. Neumann and M. Beller, *Chem. Commun*. 2011, **47**, 7959-7961.

[8] N. Dmitri, Korolev, and N. A. Bumagin, *Tetrahedron Letters*. 2005, **46,** 5751-5754.

[9] a) C. Yu, B. Tian, J. Fan, G. D. Stucky and D. Zhao, *J. Am. Chem. Soc.* 2002, **124**, 4556-4557; b) J. D. Galo, A. A. S. Illia, C. Sanchez, B. Lebeau and J. Patarin, *Chem. Rev.* 2002, **102**, 4093-4138.

[10] M. D. Alba, Z. Luan and J. Klinowski, *J. Phys. Chem*.1996, **100**, 2178-2182; b) A. B. Bourlinos, T. Karakoatas and D. Petridis, *J. Phys. Chem. B*. 2003, **107,** 920-925.

[11] Y. Jiang, Q. Gao, H. Yu, Y. Chen and F. Deng. *Micro. Meso. Mat*. 2007, **103**, 316-324.

[12] M. Kaplun, A. Nordin and P. Persson, *Langmuir*. 2008, **24**, 483-489.

[13] H. Yoshitake, T. Yokoi and T. Tatsumi, *Chem. Mater*. 2002, **14,** 4603-4610.

[14] P. Chidambaram and A. P. Singh, *App. Cat. A: Gen*. 2006, **310**, 79-90.

[15] D.S. Shephard, W. Zhou, T. Maschmeyer, J.M. Matters, C.L. Roper, S. Parsons, B.F.G. Johnson, and M. J. Duer, *Angew Chem.Int. Ed.* 1998, **37,** 2719-2723.

[16] A. Gniewek, A. M. Trzeciak, J. J. Ziółkowski, L. K. epinski, J. Wrzyszcz, and W. Tylus, *J. Catal*. 2005, **229**, 332-343.

[17] Z. Gao, Y. Feng, F. Cui, Z. Hua, J. Zhou, Y. Zhu and J. Shi, *J. Mol. Cat. A: Chem.* 2011, **336,** 51-57.

[18] D.S. Martin, R.M. Rush and G.A. Robin, *Inorg. Chem.* 1980, **19,** 1705-1709.

[19] a) M. M. Manas, M. Perez and R. Pleixats, *J. Org. Chem.* 1996, **61**, 2346-2351; b) N. Miyaura, K. Yamada, H. Suginome and A. Suzuki *J. Am. Chem. Soc.* 1985, **107,** 972-980.

[20] B. Zhang, J. Song, H. Liu, J. Shi, J. Ma, H. Fan, W. Wang, P. Zhang and B. Han. *Green chem.* 2014, **16**, 1198-1201.

[21] T. Ljungdahl, T. Bennur, A. Dallas, H. Emtenas and J. Mårtensson. *Organometallics*. 2008, **27**, 2490-2498; b) T. Ljungdahl, K. Pettersson, B. Albinsson and J. Mårtensson, *J. Org. Chem*. 2006, **71**, 1677-1687.

[22] a) J. Cheng, Y. Sun, F. Wang, M. Guo, J. H. Xu, Y. Pan and Z. Zhang. *J. Org. Chem.* 2004, **69**, 5428-5432; b) B. H. Lipshutz, D. W. Chung and B. Rich. *Org. lett*. 2008, **10**, 3793-3796.

[23] D. Zhao, J. Feng, Q. Huo, N. Melosh, G. Fredrickson, B. Chmelka and G. Stucky, *Science* 1998, **279**, 548–552.

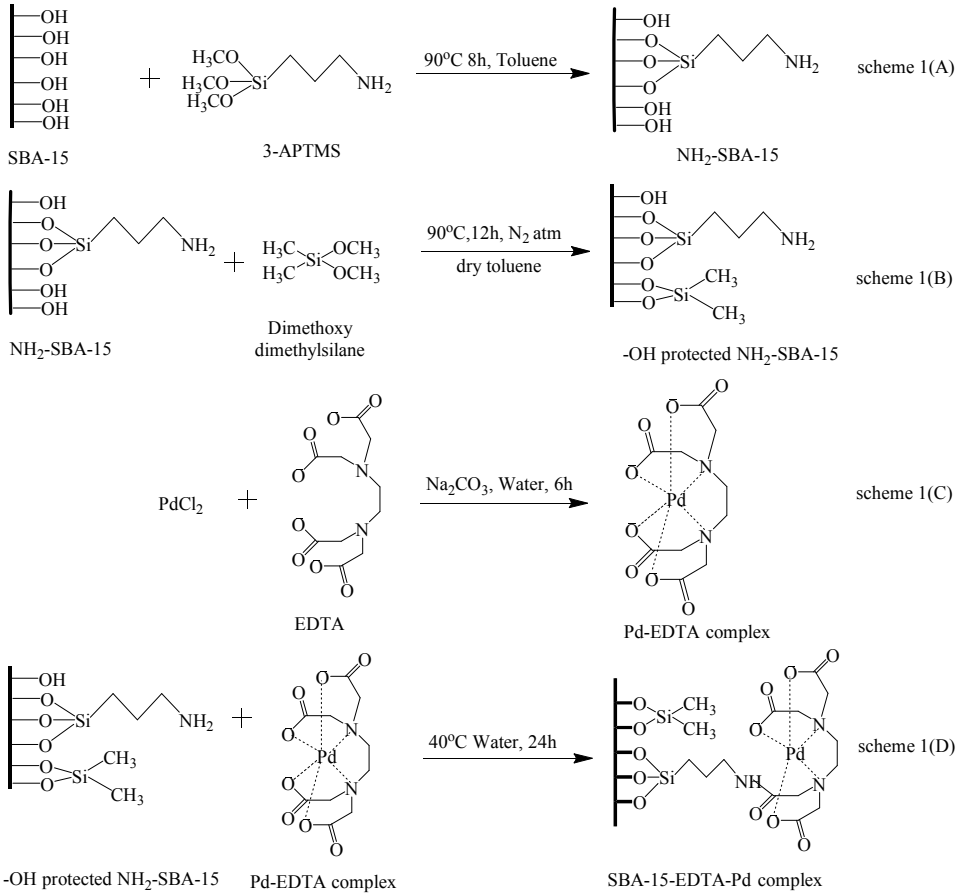

Scheme 1. Schematic diagram of SBA-15 Functionalization and heterogenization of Pd-EDTA-SBA-15. 1(A) Amino(-NH_2) functionization, 1(B) Capping of SBA-15, 1(C) Pd-EDTA complex Formation, 1(D) anchoring of Pd-EDTA complex over modified surface of SBA-15.

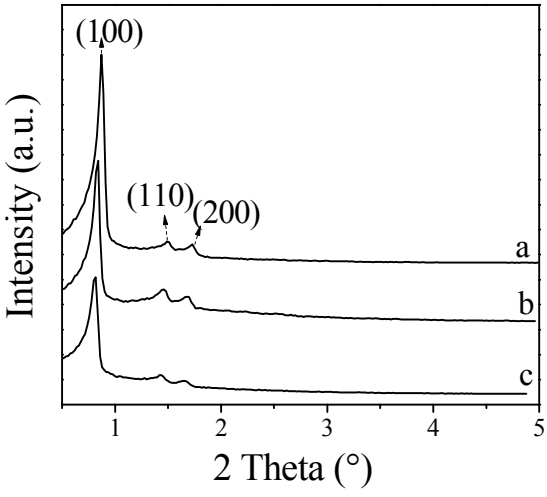

Figure 1. XRD pattern of (a) calcined SBA-15 (b) -OH protected -NH_2-SBA-15 (c) SBA-15-EDTA-Pd(11).

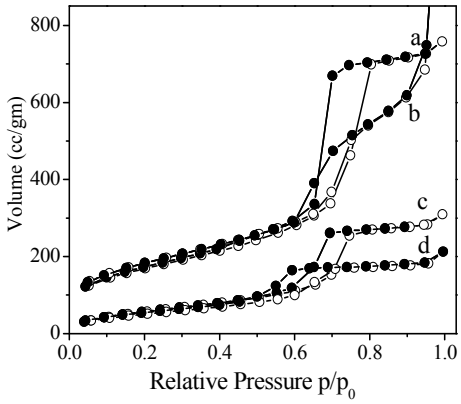

Figure 2. Nitrogen adsorption-desorption isotherm of (a) calcined SBA-15, (b) SBA-15-EDTA-Pd (7), (c) SBA-15-EDTA-Pd(11), (d) SBA-15-EDTA-Pd(15).

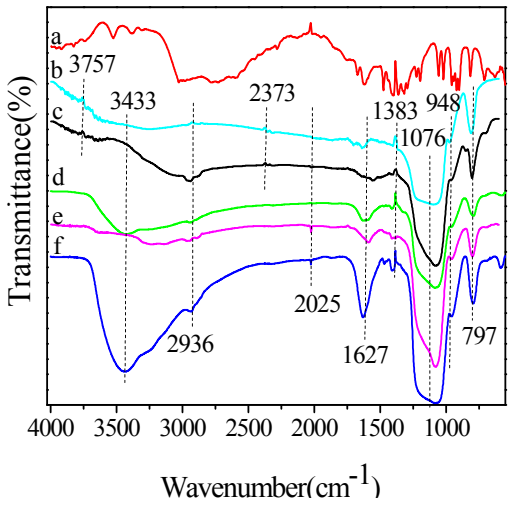

Figure 3. FT-IR spectrum of (a) EDTA, (b) calcined SBA-15, (c) –OH protected NH_2-SBA-15, (d) SBA-15-EDTA-Pd(7), (e) SBA-15-EDTA-Pd(11), (f) SBA-15-EDTA-Pd(15).

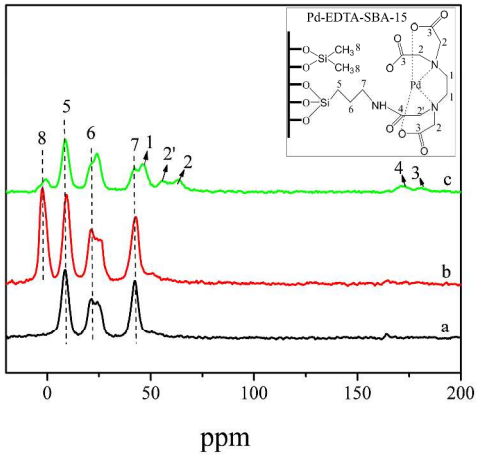

Figure 4. Solid state ^{13}C CP/MAS NMR spectrum of (a) NH_2-SBA-15, (b)-OH protected -NH_2-SBA-15 (c) SBA-15-EDTA-Pd(11).

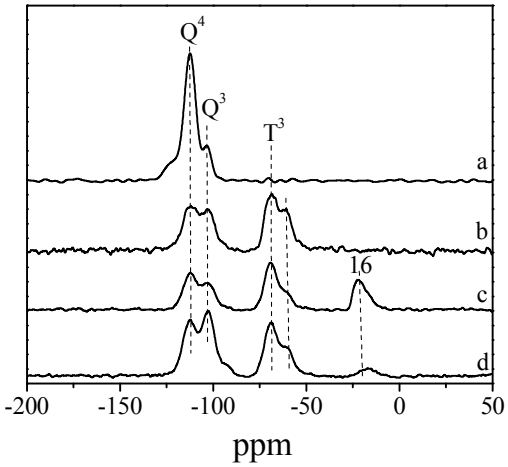

Figure 5. Solid state ^{29}Si CP/MAS NMR spectrum of (a) Calcined SBA-15, (b) NH_2-SBA-15, (c)-OH protected -NH_2-SBA-15 (d) SBA-15-EDTA-Pd(11).

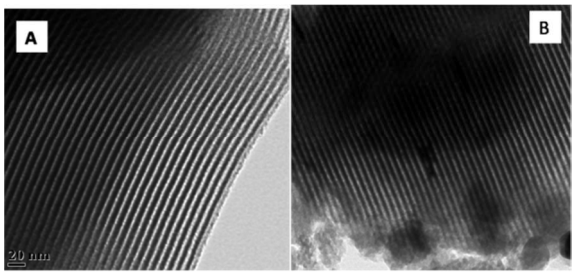

Figure 6. TEM Images of calcined (A) SBA-15 and (B) SBA-15-EDTA-Pd(11).

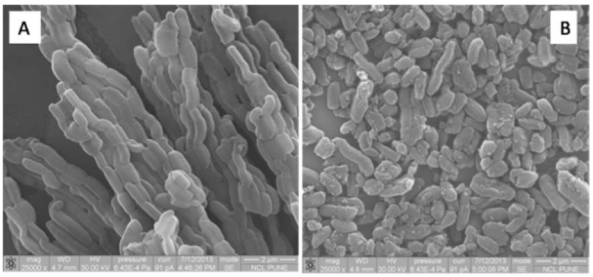

Figure 7. SEM Images of calcined (A) SBA-15 and (B) SBA-15-EDTA-Pd(11).

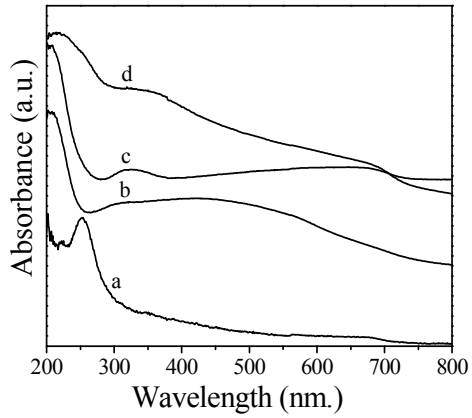

Figure 8. UV absorbance spectra of (a) Calcined SBA-15, (b) SBA-15-EDTA-Pd(7), (c) SBA-15-EDTA-Pd(11), (d) SBA-15-EDTA-Pd(15).

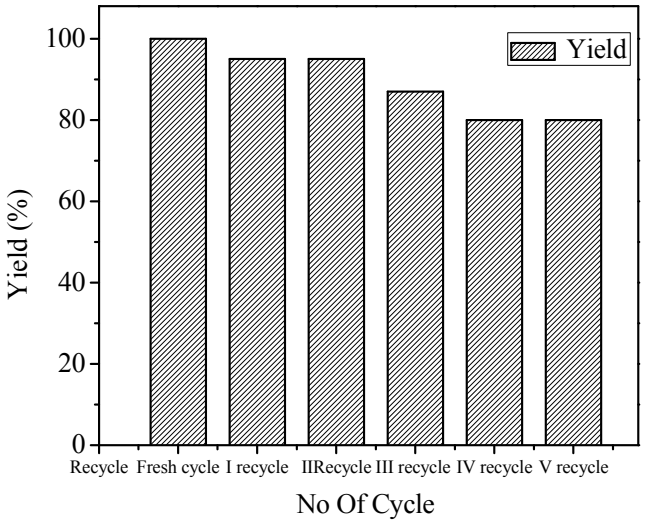

Figure 9. Recycling study of SBA-15-EDTA-Pd(11) catalyst.

Table 1. Textural properties of mesoporous calcined SBA-15 & SBA-15-EDTA-Pd.

Sample	N (wt. %) (a)	Loading of Pd (wt. %) (b)		BET surface area (m^2/g)	Average pore diameter (D_P) (Å)	Pore volume (V_p, cm^3/g)
		Input	Output			
Calcined SBA-15				739	65	1.17
SBA-15-EDTA-Pd(7)	2.2	7	5.7	665	64	0.43
SBA-15-EDTA-Pd(11)	2.5	11	6.2	363	56	0.47
SBA-15-EDTA-Pd(15)	4.3	15	10.8	187	48	0.36

[a] Calculated based on elemental (Nitrogen) analysis value.

[b] Input is based on the amount of Pd during synthesis reaction; output is based on the ICP-OES analysis.

Table 2. Reactivity of SBA-15-EDTA-Pd(11) catalyst for Suzuki reaction

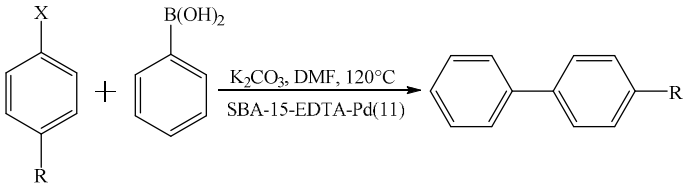

Arylhalide phenyl boronic acid Biphenyl

S.No	Aryl halide	Product	Time (h)	Yield (%)	TON
1	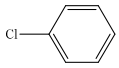	2a 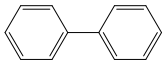	30	71	81
2	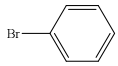	2a 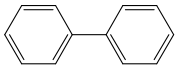	8	83	94
3	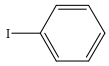	2a 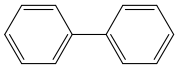	5	98	128
4.	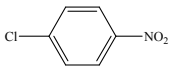	2b 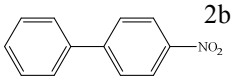	6	98	128
5.	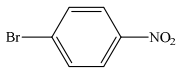	2b 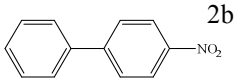	6	99	130
6.	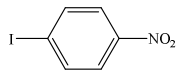	2b 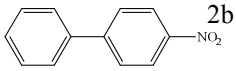	3	95	125
7.	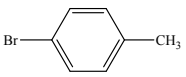	2c 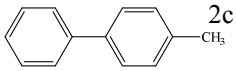	9	96	109
8.	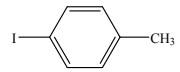	2c 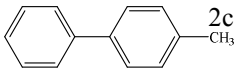	7	94	107
9.	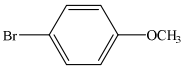	2d 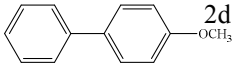	9	89	101
10.	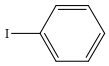	2a 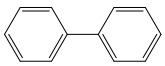	1	99#	130

Reaction conditions: (1.5 mmol) arylboronic acid, (1 mmol) Aryl halide, (3 mmol) potassium carbonate (base), 3.5 ml DMF with (15 mg) Heterogeneous SBA-15-EDTA-Pd(11) catalyst, temperature 120°C.

Carried out in homogeneous catalyst EDTA-Pd. (3 mol %)

Table 3. Reactivity of SBA-15-EDTA-Pd(11) catalyst for Sonogashira reaction

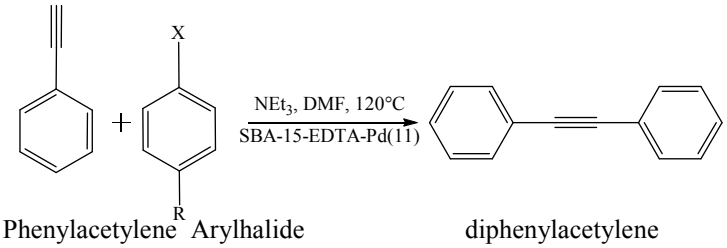

Phenylacetylene Arylhalide diphenylacetylene

S. No	Aryl halide	Product	Time (h)	Yield (%)	TON
1	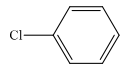	3a 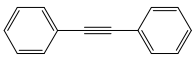	24	75	85
2	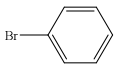	3a 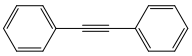	8	85	97
3	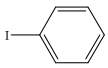	3a 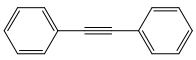	6	100	114
4.	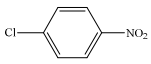	3b 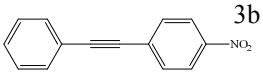	1	99	113
5.	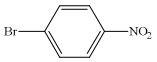	3b 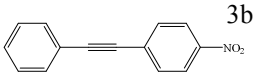	7	98	112
6.	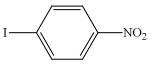	3b 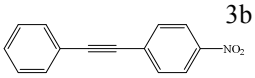	1	100	114
7.	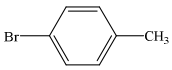	3c 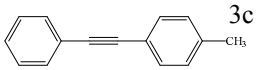	9	89	101
8.	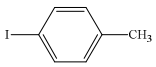	3c 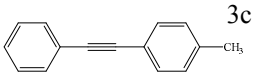	7	99	113

Reaction conditions: (1.15 mmol) Phenyl acetylene, (1 mmol) aryl halide, (3 mmol) triethylamine (base), 3.5 ml DMF with (15 mg) heterogeneous SBA-15-EDTA-Pd(11) catalyst, temperature 120°C.

Table of content

Phosphine free SBA-15-EDTA-Pd highly active recyclable catalyst: Synthesis Characterization and application for Suzuki and Sonogashira reaction.

Priti Sharma and A.P.Singh

A.P.Singh
Catalysis Division
CSIR-National Chemical Laboratory
Pune 411008, India
Fax: (+) 91 20 2590 2633
Tel: (+) 91 20 2590 2497
E-mail: ap.singh@ncl.res.in (Dr. A. P. Singh)

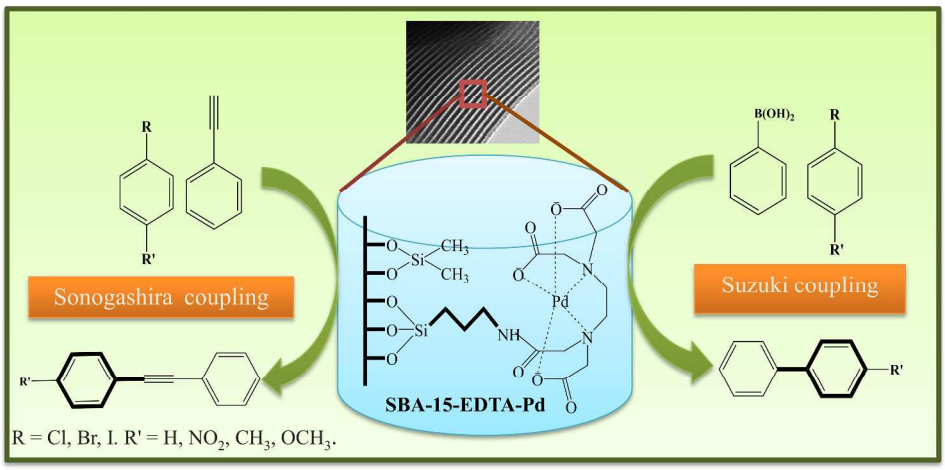

SBA-15-EDTA-Pd(11) was demonstrated highly efficient and reusable heterogeneous catalyst for Suzuki and Sonogashira reaction in phosphine and co-catalyst free reaction condition.